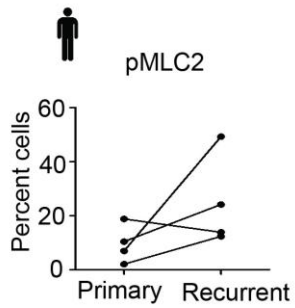


In the format provided by the authors and unedited.

A tension-mediated glycocalyx-integrin feedback loop promotes mesenchymal-like glioblastoma

J. Matthew Barnes^{1,14}, Shelly Kaushik^{1,14}, Russell O. Bainer¹, Jason K. Sa^{2,3}, Elliot C. Woods⁴, FuiBoon Kai¹, Laralynne Przybyla¹, Mijeong Lee^{2,5}, Hye Won Lee^{2,6}, Jason C. Tung¹, Ori Maller¹, Alexander S. Barrett⁷, Kan V. Lu⁸, Jonathon N. Lakins¹, Kirk C. Hansen⁷, Kirsten Obernier^{8,9}, Arturo Alvarez-Buylla^{8,9}, Gabriele Bergers^{8,10}, Joanna J. Phillips⁸, Do-Hyun Nam^{2,5,11}, Carolyn R. Bertozzi⁴ and Valerie M. Weaver^{1,9,12,13*}

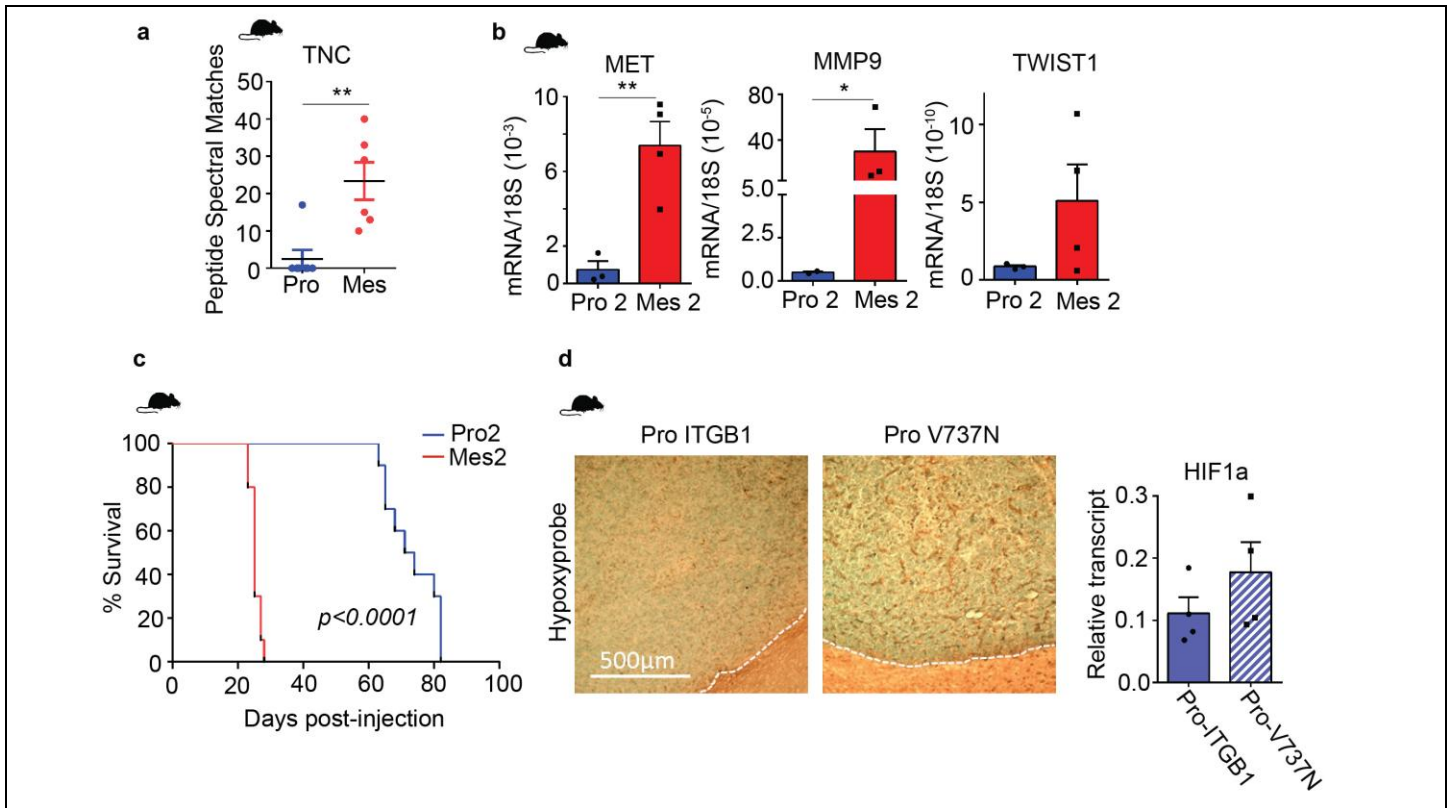
¹Center for Bioengineering and Tissue Regeneration, Department of Surgery, University of California San Francisco, San Francisco, CA, USA. ²Institute for Refractory Cancer Research, Samsung Medical Center, Seoul, Korea. ³Research Institute for Future Medicine, Samsung Medical Center, Seoul, Korea. ⁴Department of Chemistry and Howard Hughes Medical Institute, Stanford University, Stanford, CA, USA. ⁵Department of Health Sciences and Technology, SAIHST, Sungkyunkwan University, Seoul, Korea. ⁶Department of Anatomy and Cell Biology, Sungkyunkwan University School of Medicine, Suwon, Korea. ⁷Department of Biochemistry and Molecular Genetics, University of Colorado, Denver, Aurora, CO, USA. ⁸UCSF Department of Neurological Surgery, Helen Diller Cancer Center, University of California San Francisco, San Francisco, CA, USA. ⁹Eli and Edythe Broad Center of Regeneration Medicine and Stem Cell Research, University of California, San Francisco, San Francisco, CA, USA. ¹⁰Vlaams Instituut for Biotechnologie-Center for Cancer Biology and KU Leuven, Leuven, Belgium. ¹¹Department of Neurosurgery, Samsung Medical Center, Sungkyunkwan University School of Medicine, Seoul, Korea. ¹²UCSF Comprehensive Cancer Center, Helen Diller Family Cancer Research Center, University of California San Francisco, San Francisco, CA, USA. ¹³Department of Anatomy, Department of Bioengineering and Therapeutic Sciences and Department of Radiation Oncology, University of California San Francisco, San Francisco, CA, USA. ¹⁴These authors contributed equally: J. Matthew Barnes, Shelly Kaushik. *e-mail: valerie.weaver@ucsf.edu



Supplementary Figure 1

Increased mechanical signaling in recurrent versus primary GBM

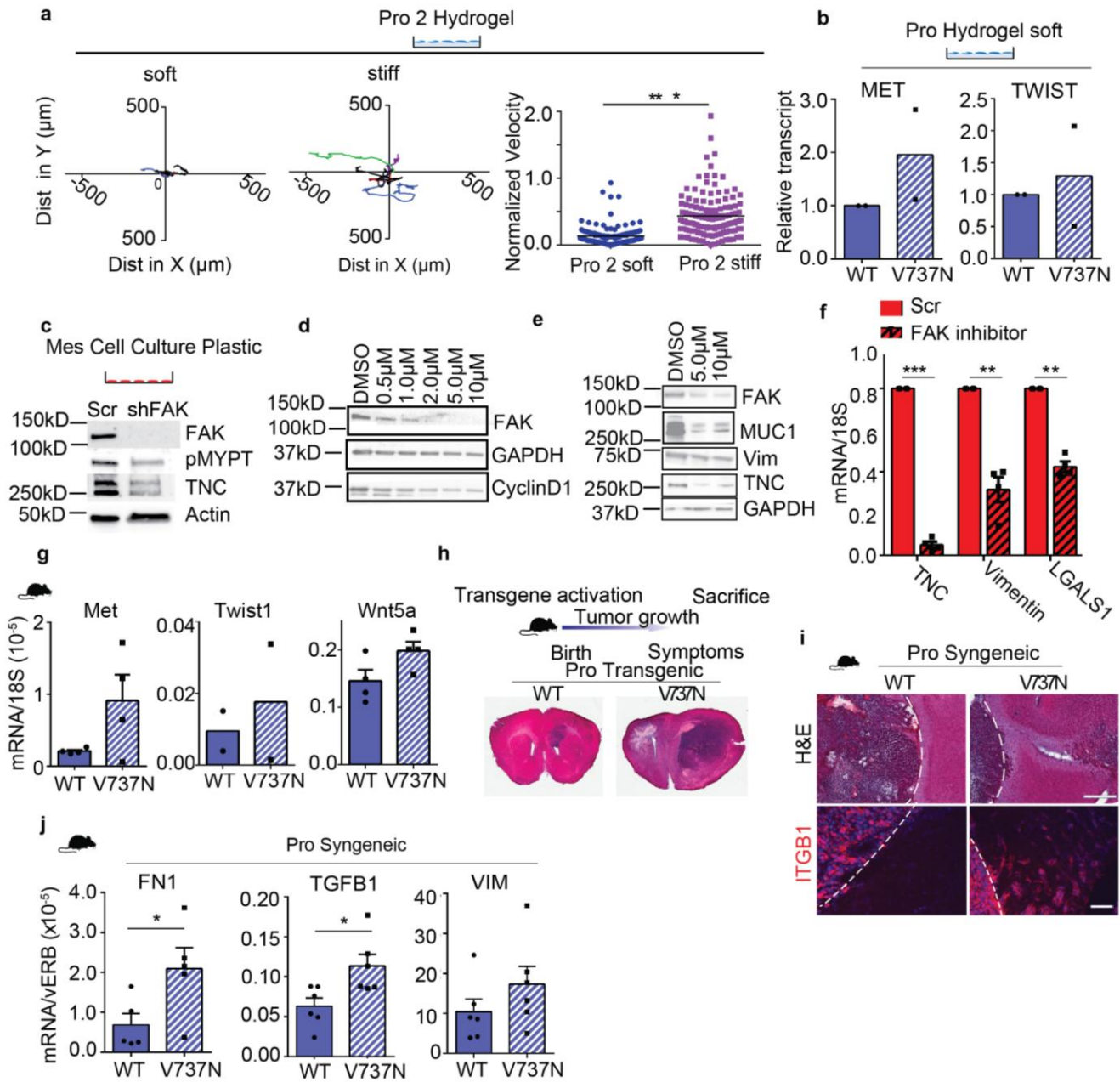
Quantification of cells expressing pMLC2 in four paired primary and recurrent GBM patient samples (Nam cohort); Quantification was performed by calculating the percent of cells expressing phospho myosin light chain 2 (pMLC2), stained in red, the representative image for which is shown in Figure 1a, in four primary and recurrent GBM patient samples, using multiplex immunohistochemistry.



Supplementary Figure 2

Increased mesenchymal-ness is associated with GBM aggression

a, Mass spectrometry analysis of human pro and mes GBM xenografts; n=7 pro and 6 mes xenograft samples; mean \pm sem; **p=0.009, by two-sided Mann Whitney U-test. **b**, RNA from additional proneural 2 (pro2) and mesenchymal 2 (mes2) patient-derived tumor xenografts was analyzed by qPCR; n=3 mice/group for GBM12 and 4 mice/group for GBM10; mean \pm sem; *p=0.008, 0.02 and 0.18 for Met, MMP9 and TWIST1 respectively by two-sided unpaired t-test. **c**, Kaplan Meier analysis of nude mice injected with human pro 2 and mes 2 GBM cells; n=10 mice/group; p-value by two-sided logrank test result shown on plots. **d**, Representative image (left) and quantification (right) of hypoxia using the hypoxyprobe and HIF1 α transcript levels in control vs V737N pro xenograft mice; mean \pm sem; n=4 mice/group; p=0.34 by two-sided Mann Whitney-U test.

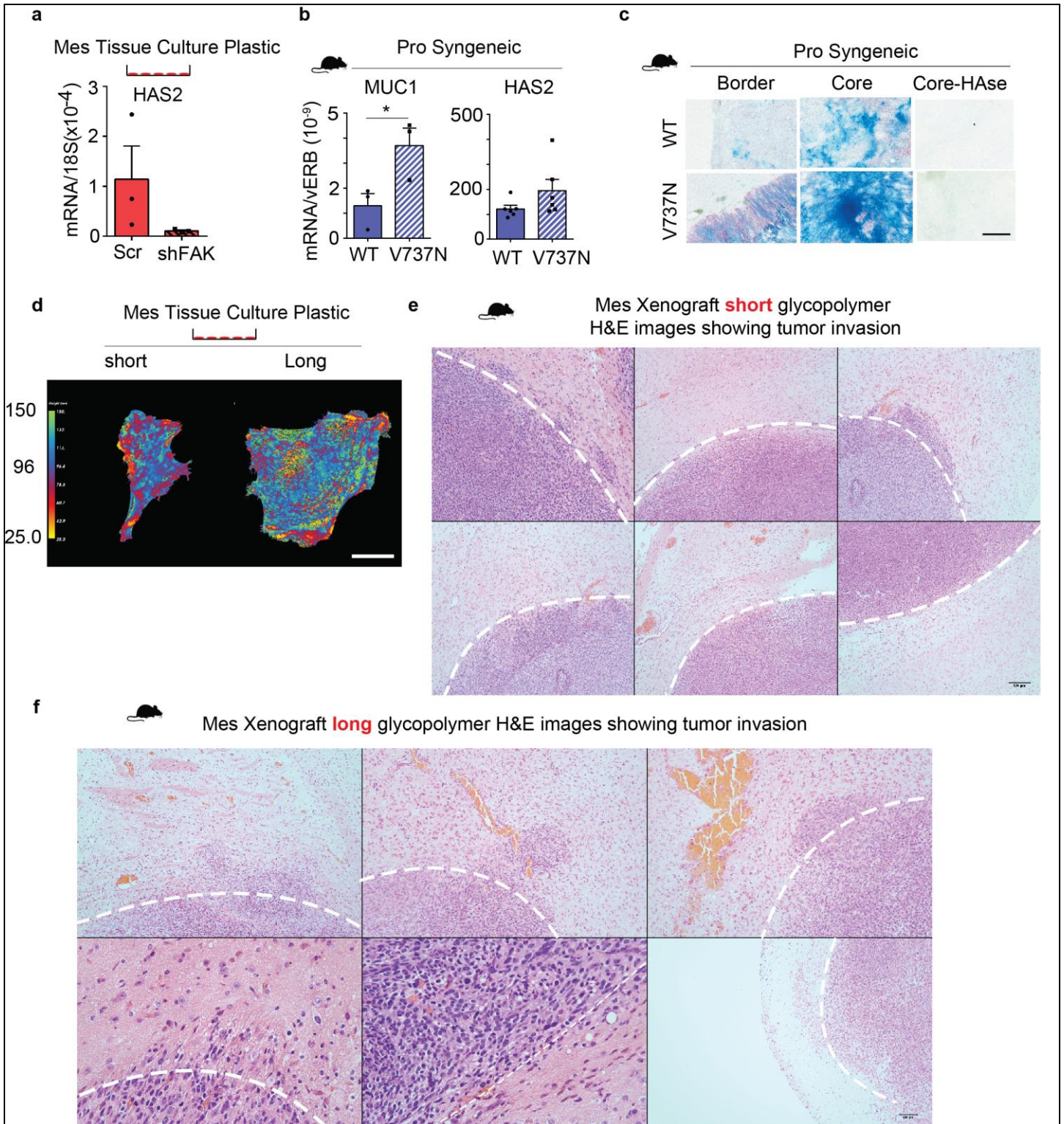


Supplementary Figure 3

Enhanced mechanosignaling induces a mesenchymal-like phenotype in GBM

a, PRO 2 cells were imaged on soft and stiff polyacrylamide hydrogels for 36 hours. Migration tracking was performed and velocity calculated using Manual Tracker on Image J; n=9 cells for soft and n=6 stiff conditions from three independent experiments; each point on the velocity plot (right) was derived from calculating distance/time/frame where n=132 frames/condition averaged over 9 and 6 cells on soft and stiff respectively pooled from 3 independent experiments; mean \pm sem; * $p=1.13 \times 10^{-16}$ by a two-sided paired t-test. **b**, qPCR analysis of wildtype and V737N cells on soft hydrogels for expression of mesenchymal markers from two independent experiments; data show the mean of two independent experiments. **c**, Lysates from mes control

(scr) and FAK knockdown (shFAK) cells were analyzed for FAK transcript knockdown from two independent experiments. **d and e**, Immunoblotting of mes cells treated with increasing doses of FAK inhibitor (left). Mes cells treated with FAK inhibitor at indicated concentrations were lysed and analyzed for the indicated markers (right); representative of 2 experiments. **f**, RNA from mes cells treated with FAK inhibitor was analyzed for indicated markers; mean \pm sem; n= 4 independent experiments; p=0.00012, p= 0.007 and 0.002 for TNC, vimentin and LGALS1 respectively using two-sided unpaired t-test. **g**, qPCR analysis for markers of mesenchymal-ness in wild-type and V737N xenografted tumors; n=2 mice/group for Twist1 and 4 mice/group for all else; mean \pm sem. **h**, Top: model of transgenic tumor growth. Bottom: representative H&E staining of WT and V737N transgenic tumors; n=4 mice/group. **i**, WT and V737N mouse cells were derived from lentiviral transfection of the transgenic WT E/p53 tumor cells and injected into FVB/n hosts. Tumors stained for H&E and human integrin β 1 (ITGB1), only expressed in cells expressing WT or V737N transgene; dashed line delineates tumor from normal brain; n=3 mice/group; scale bar 400 μ m for H&E (top) and 50 μ m for IF (bottom). **j**, RNA from pro syngeneic tumors was analyzed via qPCR; n=5 animals/group for FN1 and 6 animals/group for all else; mean \pm sem; *p= 0.032, 0.03 and 0.18 by two-sided Mann Whitney-U test. Source data in Supplementary Table 4.

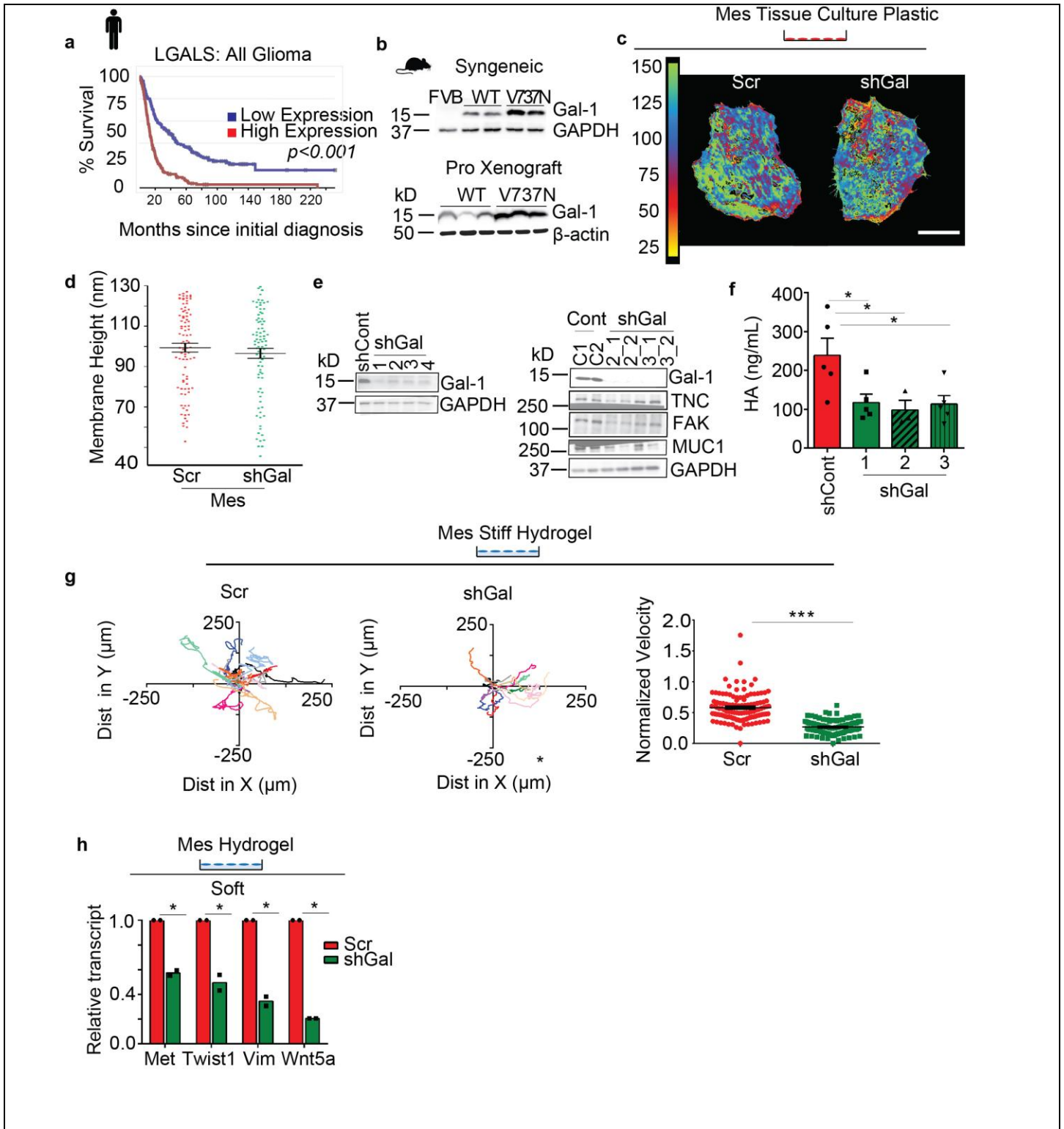


Supplementary Figure 4

Enhanced mechanical signaling in mesenchymal tumors increases the glycoalyx bulkiness

a, qPCR analysis of HAS2 transcript levels in control mes scr vs shFAK mes cells. $n=3$ samples/group; mean \pm sem; p -value = 0.3 by two-sided paired t-test. **b**, RNA from WT and V737N pro syngeneic tumors analyzed by

qPCR; n=3 and 6 mice/group for MUC1 and Has2; mean \pm sem; *p=0.046 and 0.14 for MUC1 and Has2 respectively by two-sided unpaired t test. **c**, Alcian Blue staining of WT and V737N pro syngeneic tumor sections with and without hyaluronidase (HAse) treatment (1mg/mL for 30 minutes at 37C, control samples held at 37C for 30 minutes in PBS), scale bar 250 μ m, representative of 3 samples per group. This experiment indicates the majority of Alcian Blue staining in these tumors is due to HA-binding. **d**, Representative SAIM image of mes GBM cells loaded with short (3nm) or long (90nm) glycopolymers; scale bar 10 μ m; n=24 and 23 measurements for short and long glycopolymers respectively; quantification shown in Fig. 5e. **e and f**, Images of long and short glycopolymer decorated tumors. White lines represent delineation of tumor-normal brain boundary; n=4 mice, representative images and quantification shown in Fig. 4h; Scale bar 400 μ m.

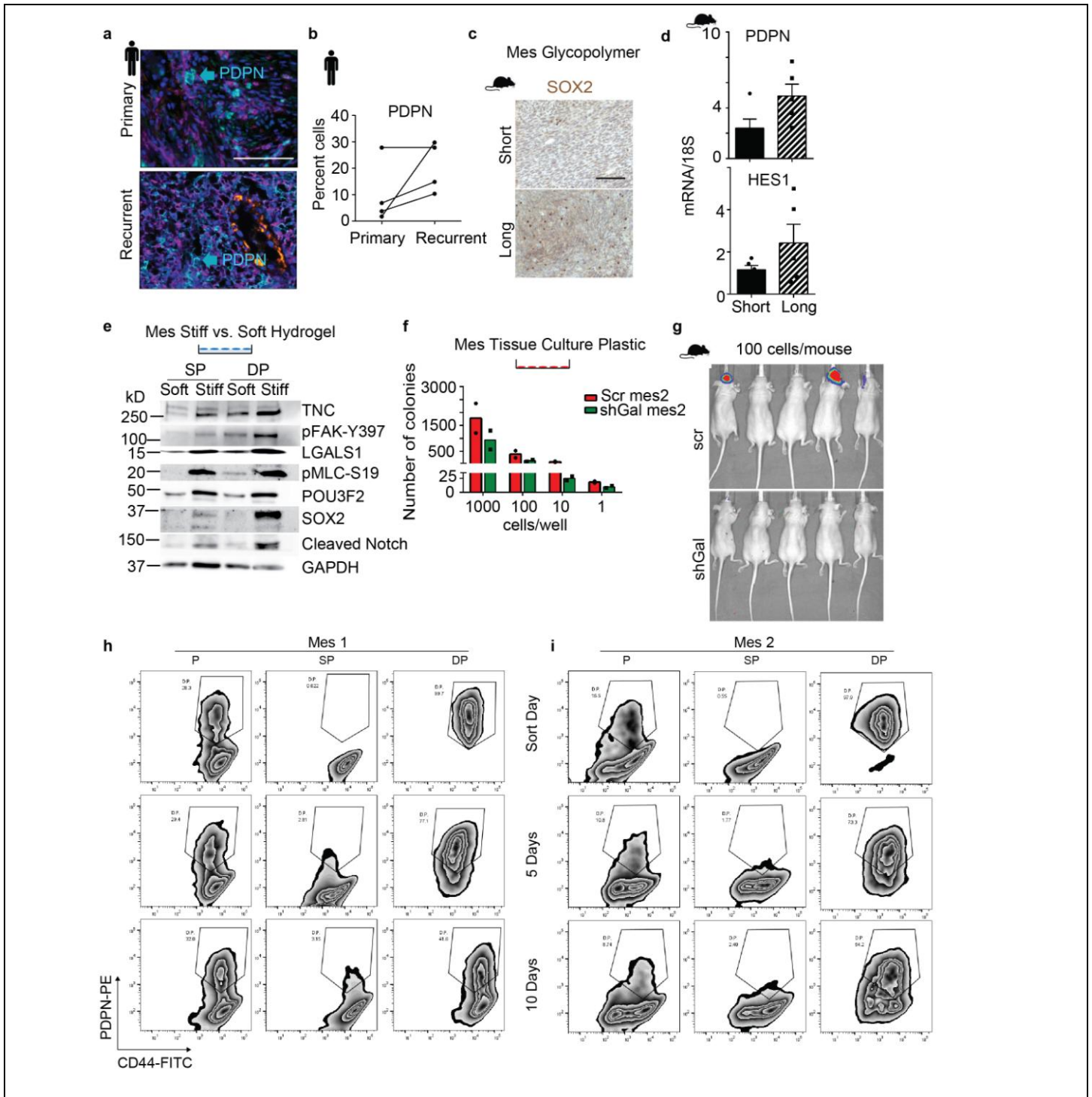


Supplementary Figure 5

Galectin-1 regulates mechanical and mesenchymal phenotype in GBM

a, Kaplan Meier analysis of Rembrandt data showing percent survival probability vs. expression level of Gal-1

in all glioma patients; n=214 GBM, 66 oligo and 145 astro; p-value by two-sided logrank test. **b**, Immunoblotting of lysates from WT and V737N syngeneic (top) and pro xenograft (bottom) tumors for Gal-1 protein n=3 tumors/group for xenograft, 2 tumors/group for syngeneic, FVB=normal cortex lysate. **c**, Glycocalyx height was measured in mes scr and shGal-1 GBM cells by scanning angle interference microscopy (SAIM); scale bar 10 μ m; representative of three independent experiments. **d**, Scatter plot on right is derived from four independent experiments, mean \pm sem; each point represents measurement of glycocalyx height/frame; n=91 and 90 measurements over 10 cells for scr and shGal-1 respectively; p=0.17 by two-sided paired t-test. **e**, Immunoblot shows knockdown of Galectin-1 using additional shGal hairpins. shGal (1) is the main hairpin used for all *in vitro* and *in vivo* studies (clone#TRCN0000057423, Sigma Aldrich). shGal clones (2), (3) and (4) are additional hairpins validated for knockdown (clones#TRCN0000057424, TRCN0000057425 and TRCN0000057427, Sigma Aldrich). Immunoblot (left) shows validation of Galectin-1 knockdown. Immunoblot (right) shows effects on TNC, FAK, MUC1 upon Galectin-1 knockdown with clones (2) and (3); n=2 independent experiments/clone. **f**, Hyaluronic acid production was measured from cell supernatants expressing shGal-1 clones (1), (2) and (3); n=3 independent experiments for shGal (2) and 5 independent experiments for all others; *p=0.037, 0.033 and 0.034 for shGal clones (1), (2) and (3) respectively. **g**, Mes scr and shGal cells were plated on stiff hydrogels and imaged over 36 hours. Migration tracking (left) was performed using Manual Tracker; n=12 cells/condition from three independent experiments. Velocity plot (right) was derived from calculating distance/time/frame where n=120 frames/condition averaged over 12 cells; mean \pm sem; ***p= 1.5×10^{-28} by two-sided paired t-test. **h**, qPCR analysis for markers of mesenchymal-ness for RNA from scr vs shGal cells on soft hydrogels; n=2 independent experiments; source data in Supplementary Table 4.

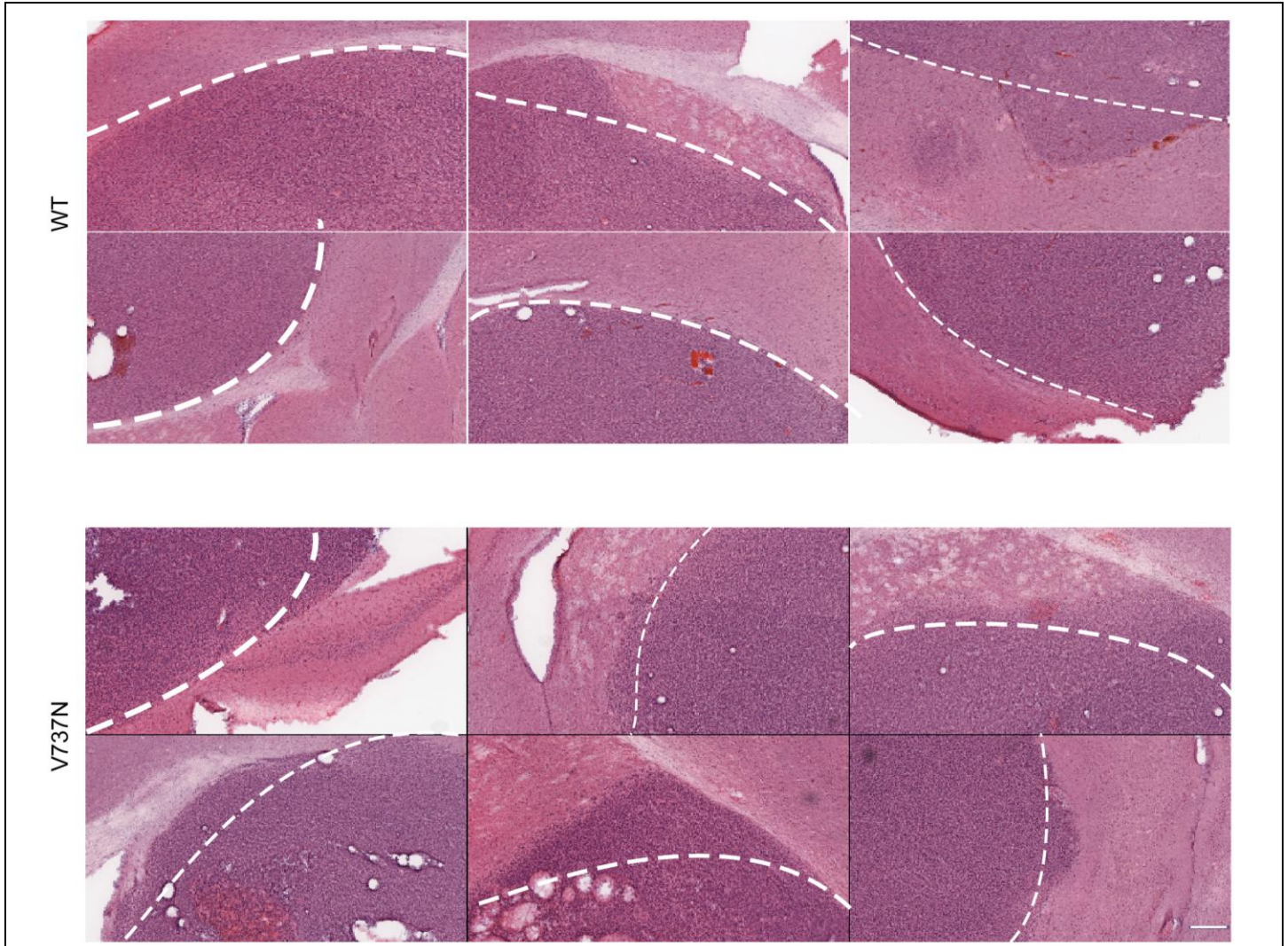


Supplementary Figure 6

A bulky glyocalyx promotes a stem-like phenotype in mesenchymal GBM

a, Representative images of four paired human primary and recurrent patient samples (Nam cohort) stained for PDPN using multiplex IHC; Blue arrows indicate regions of PDPN expression; scale bar 50 μ m. **b**, Cells from Supplemental Fig. 6a expressing PDPN were quantified in primary vs recurrent tumors; n=4 patients per group. **c**, SOX2 in short and long Mes glycopolymer tumor sections; representative of 4 mice/group; scale bar 100 μ m.

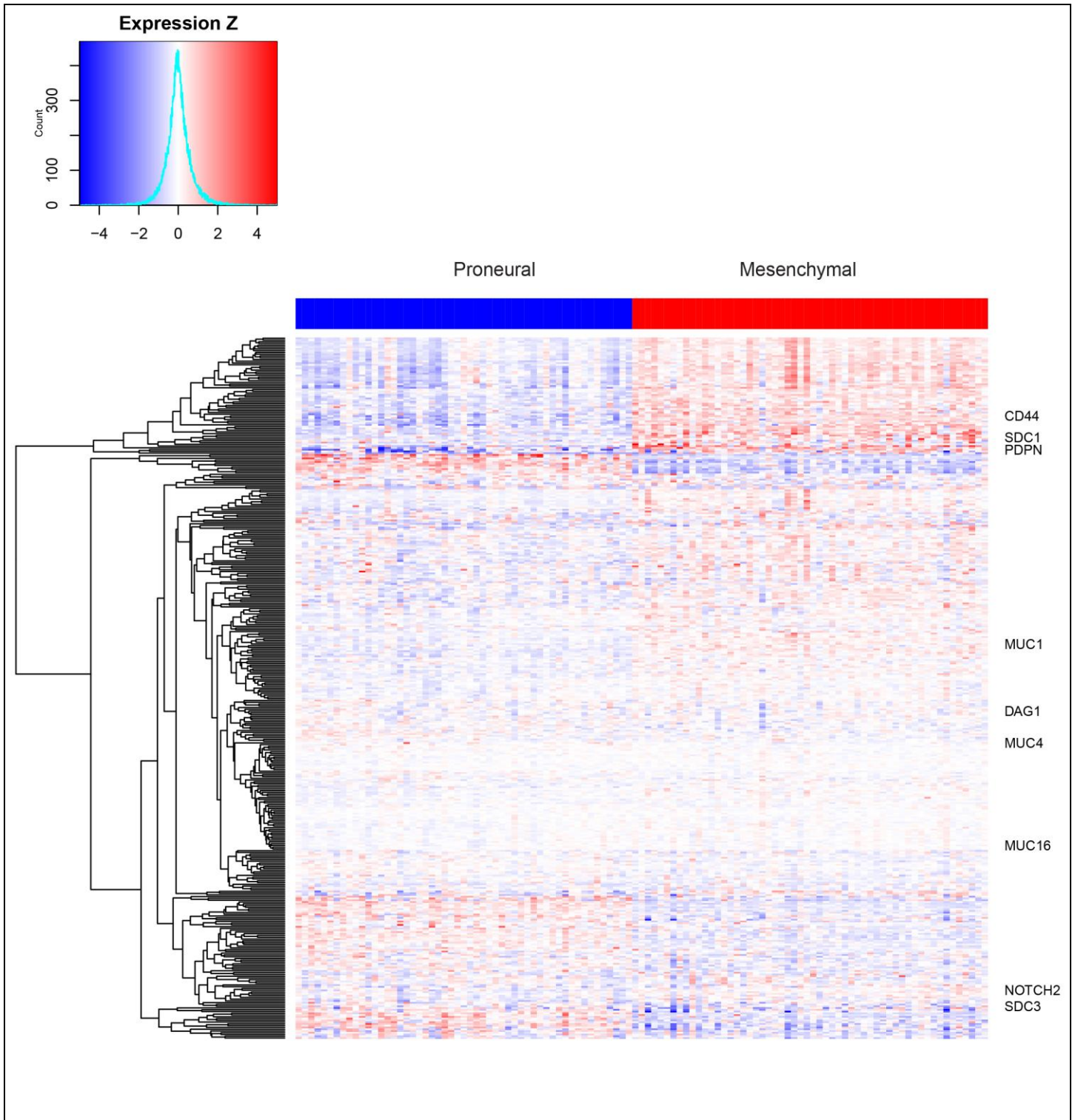
d, RNA from short and long Mes glycopolymer tumors was analyzed via qPCR; mean \pm sem; n=5 mice/group; p=0.06 and 0.2 for PDPN and Hes1 respectively by two-sided unpaired t-test. **e**, FACS was used to isolate CD44:podoplanin DP, CD44 single positive (SP) cells, cultured on soft or stiff hydrogels for 18 hours prior to lysis for immunoblot of the indicated markers; n=3 independent experiments. **f**, *In vitro* limiting dilution assays were performed for additional mes control (scr mes2) vs gal-1 knockdown cells (shGal mes2) for the cells numbers indicated; n= 2 independent experiments. **g**, *In vivo* limiting dilution assays were performed for mesenchymal control (Scr) vs shGal cells injected into nude mice at the rate of 100 cells/mouse. The image shows the number of non-tumor-bearing and tumor-bearing mice at the study endpoint. Quantification shown in Fig. 6m. **h and i**. FACS analysis of PDPN and CD44 in DP, SP, and parental (unsorted cells) populations from Mes1 and Mes2 primary GBMs immediately after the sort (“sort day”), and 5 and 10 days after the sort. The images are representative of three independent sorts. Source data in Supplementary Table 4.



Supplementary Figure 7

Increased local invasion in V737N expressing tumors

Representative images of pro ITGB1 and V737N overexpressing tumors. White lines represent delineation of tumor-normal brain boundary; n=4 mice per condition, representative images and quantification shown in Fig. 2j; Scale bar 400 μ m.



Supplementary Figure 8

Heatmap of bulky genes differentially expressed in proneural and mesenchymal human GBM patients

Heat map of “bulky genes” found to be differentially expressed in proneural versus mesenchymal tumors. Few bulky genes of interest listed for simplification. A comprehensive list is available in supplemental table 1.

Figure 2g

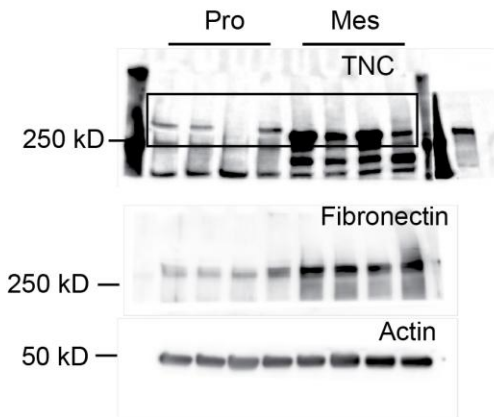


Figure 3b

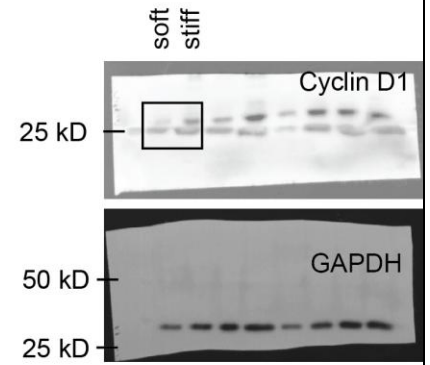
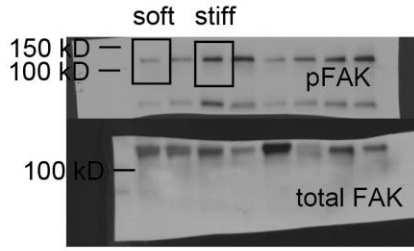


Figure 5f

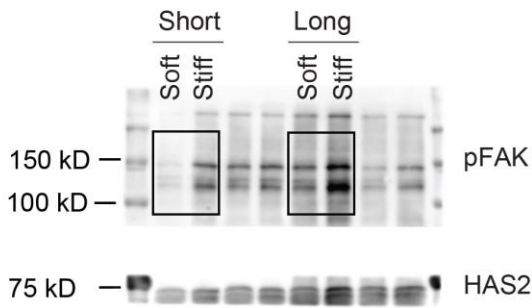
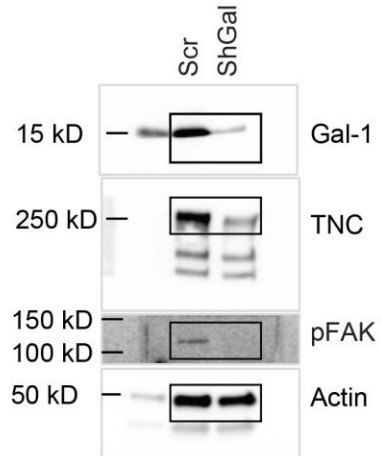


Figure 6i



Supplementary Figure 9

Full scans of key blots

Unprocessed western blots for Figures 2g, 3b, 5f and 6i

Supplementary Table 1: Bulky Genes List. A list of genes characterized as “bulky” based on their putative O- and N- glycosylation patterns. The table shows bulky genes for violin plots in Figs 4a and 4c, as well as the genes for Kaplan Meier analysis in Figs 1e and 4b.

Supplementary Table 2: Primer sequences. A list of all the primers used for qPCR analysis, along with their forward and reverse sequence information

Supplementary Table 3: Antibody information. A list of all the antibodies used in this study (western blot, immunohistochemistry, immunofluorescence and flow cytometry) and information regarding these antibodies, including catalog number, company, clone and lot numbers, and their method of validation.

Supplementary Table 4: Statistics source data. The source data is included for all the figures where individual experiments were repeated twice (Figs 3e, 3h, 5e, 6h and 7g; supplementary figures S3b, S3g S5h and S6f). Each tab represents data (two experiments, depicted as n=1 and n=2) for a single figure panel, along with individual raw data points per repeat.